Magnesium Technology 2013
Edited by: Norbert Hort, Suveen N. Mathaudhu, Neale R. Neelameggham, and Martyn Alderman
TMS (The Minerals, Metals & Materials Society), 2013

THE TEXTURE AND MICROSTRUCTURE EVOLUTION OF Mg-Zn-Ce ALLOYS

M. Sanjari[1], A. Farzadfar[1], T. Sakai[2], H. Utsunomiya[2], E. Essadiqi[3], In-Ho Jung[1], S.Yue[1]
[1]Department of Materials Engineering, McGill University, Montreal, Canada H3A 2B2
[2] Division of Materials and Manufacturing Science, Graduate School of Engineering, Osaka University
[3] Université Internationale de Rabat (UIR) Technopolis, Rabat Morocco

Keywords: Rare-earth elements, Rollability, Texture weakening

Abstract

The texture evolution in four Mg-Zn-Ce alloys was compared to that of Mg-3Al-1Zn (AZ31) alloy following rolling and subsequent isothermal annealing. All the as-cast and homogenized alloys were rolled through two stages that can be characterised as rough rolling and finish rolling, respectively. To investigate the effect of finish rolling temperature, one finish rolling pass with 65% reduction in thickness was performed at 300 °C and 450 °C. Of the studied compositions, the Mg-1Zn-1Ce, which had the highest Ce/Zn ratio, showed the weakest as-rolled texture and homogenous shear banding/twinning. Changing the Zn content changed particle size and, in alloys subject to texture weakening, the static recrystallization mechanism altered. On annealing, the maximum intensity of basal pole figures decreases as recrystallization progresses. The Mg-1Zn-1Ce (with the highest Ce/Zn), texture weakening is maintained even after full recrystallization, when grain coarsening occurs. However, in the Mg-4Zn-1Ce and AZ31 alloys, texture strengthening occurs when grain coarsening occurs, and the double split basal peak is replaced by a single peak. In these two alloys, grain coarsening is also accompanied by a bimodal grain size whereas in the Mg-1Zn-1Ce alloy, the grain coarsening leads to a uniform grain size. It is concluded that the differences between the Ce bearing alloys is related to Zn; increasing Zn decreases the solubility of Ce, which can influence the texture changes.

Introduction

The application of magnesium and magnesium alloys in the automotive industry can reduce vehicle weight, and, consequently, fuel consumption can be reduced. Sheet Mg is one way to increase the usage of Mg [1]. One of the major obstacles of its use is that a preferred crystallographic orientation (texture) develops in wrought alloys [2-4], which substantially limits the subsequent formability, especially in flat-rolled sheets [2, 5-7]. It has recently been found that the addition of rare earth (RE) elements, such as yttrium, cerium or neodymium, significantly weakens the rolling or extrusion texture of Mg alloys [4-9]. The texture weakening mechanism has been associated with different mechanism such as particle stimulated mechanism (PSN) [10, 11], deformation or shear bands containing twins [5], or retardation of dynamic recrystallization (DRX) [12]. Although the crystallographic texture evolution of Mg alloys has already been studied as a function of alloying elements and different thermomechanical processing parameters, there is still a lack of work regarding whether the RE-textures are mainly associated with changes in the deformation texture or also with changes in the recrystallization texture.

In our previous studies on Mg–Y alloy and Mg-Zn-Ce the possibility of attaining texture weakening by DRX suppression and SRX promotion was studied. It was hypothesised, in the previous work of the author, that by suppressing the DRX, the deformation cannot be accommodated in the soft DRX region; instead deformation is accommodated by compression and double twinning in basal parent grains, leading to the formation of deformation bands [24]. Despite these observations, the orientation relationship between activated deformation mechanisms and recrystallized grains remains unclear.

In this work, the nucleation and growth of recrystallized grains is studied in both as deformed and annealing state in Mg-Zn-Ce systems and compared with AZ31 as a reference alloy. In addition the effect of precipitates is investigated in the Mg-Zn-Ce alloys systems by changing the Ce and Zn contents in the alloy.

Experimental procedure

The following four alloys in the Mg-Zn-Ce system were cast into ingots of 70 mm x 110 mm x 500 mm and machined into plates 70 mm x 110 mm x 6 mm thickness:

1) Mg-1Zn-0.5Ce
2) Mg-1Zn-1Ce
3) Mg-2Zn-1Ce
4) Mg-4Zn-1Ce

The as-cast material was homogenized at 450 °C for 24 hr. To compare the results with the commercial AZ31 alloy, an AZ31 alloy with the following chemical composition (%wt): 3% Al, 0.9% Zn, 0.67% Mn and Mg (balance) was cast as a plate with 6 mm thickness and homogenized at 350 °C for 4 hr.

The rolling experiment was conducted through two steps: rough rolling and finish rolling. The purpose of rough rolling was to decrease the grain size from about 1mm to about 130 μm in preparation for high speed rolling. Rough rolling was performed at 15 m/min using a low-speed, two-high, mill with ϕ 320 mm rolls. The plates were rolled with three consecutive passes of 12-15% reduction per pass at 450 °C and the thickness reduced from 6mm to 3 mm. The samples were reheated for 10 min between each passes to keep the rolling temperature constant. After cooling in air to room temperature the rough rolled samples were annealed at 450°C for 15 min to fully recrystallize the sheet. For the finish rolling, low speed rolling (LSR) and high speed rolling (HSR) was performed in a single pass operation with reduction in thickness of about 60% at two temperatures, 300 °C and 450 °C, at rolling speeds of 15 and 1000 m/min respectively. LSR was performed in the roughing mill. HSR was performed in a two-high laboratory HSR mill with ϕ530mm rolls. Prior to finish rolling, the specimens were reheated for 10 min at the corresponding rolling temperature. Details of the experiments and the high speed rolling machines can be found in previous work [18].

The samples were cut in RD-ND planes, mounted and ground to 1200 grit and then polished with alcohol based 3 and 1 micron diamond suspensions for microstructural examination by optical microscopy. The samples were etched with an acetic-picral solution (10 mL acetic acid + 4.2 g picric acid + 10 mL water + 70 mL ethanol (99.5 pct)). The macro texture was evaluated in a Siemens D-500 X-ray diffractometer equipped with a texture goniometer using Co radiation in TD-RD plan. The data were

analyzed to calculate orientation distribution functions and to recalculate the pole figures.

Orientation imaging microscopy (OIM) was used to study grain orientation via EBSD in a Hitachi S-3000 FE-SEM at 20 kV, 70° tilt angle, and a step size between 0.3 to 0.5 µm, depending on deformation condition. For EBSD analysis, the polished samples samples were electropolished at 20 V using 10% nital solutions cooled to -10 to -30°C.

Results and discussions

Finish rolled and annealed microstructure

Figure 4 shows the microstructure of finish rolled AZ31B and Mg-Zn-Ce alloys rolled at 300°C and annealed at 450 °C for 15 min.

In terms of microstructure evolution for the AZ31B, as can be seen from Fig. 1 the as rolled structure appears to have undergone little recrystallization, revealing a 'pancaked' structure with shear bands. In this case it seems that the shear bands act as crack propagators, since only a few shear bands forms in AZ31 and strain is strongly localized in them. Macroscopic bands or shear zones have been observed in rolled magnesium, inclined to the rolling plane along surfaces that support high shear stresses, and act frequently as sites for the origin of recrystallization during subsequent annealing. It is generally found that as the temperature of deformation increases, i.e. at 450 °C, the deformation becomes more homogeneous due to an increase in the number of operating slip systems.

As can be seen in Fig. 4, in the Mg-Zn-Ce alloys, the general features of microstructure are almost the same as AZ31; the main difference is that shear bands are somewhat more difficult to observe, although in Mg-2Zn-1Ce and Mg-4Zn-1Ce the shear bands can be distinguished. However, by increasing the alloying level, the shear bands become much more difficult to discern. It seems that shear bands formed in RE-containing alloys are less intense than those formed in AZ31. The preceding studies show that the severity of shear banding is reduced when adding RE solute.

With respect to annealing, it can be seen from Fig. 1 that, in the case of AZ31, considerable recrystallization takes place, as indicated by the equiaxed structure. However addition of rare earth alloying elements has obviously changed the recrystallization behaviour and, as a general conclusion, it appears that the Mg-Zn-Ce alloys retard recrystallization. The Mg-Zn-Ce alloys (except Mg-4Zn-1Ce) start to recrystallized after 30 s (as indicated in the bottom graph of Fig. 1); however recrystallized grains can be seen in the microstructure of AZ31 and Mg-4Zn-1Ce after 30s annealing. By increasing the Zn to 4 wt% (Mg-4Zn-1Ce) the recrystallized grain size increases in this alloy compared to the alloy with lower alloying levels.

After 15 min annealing the minimum average grain size is obtained for Mg-1Zn-1Ce and larger grain sizes are obtained for AZ31 and Mg-4Zn-1Ce with the minimum Ce/Zn ratio.

Deformation Texture of rough and finish rolled sheets

The initial texture of the finish rolled samples is depicted in Fig. 2. In the case of AZ31 at 300 °C the samples shows the typical basal texture of rolled Mg alloys, with the majority of c-axes of the grains aligned with the ND. However, by increasing the temperature to 450 °C the PF slightly elongates along the RD and the maximum intensity slightly decreases. All the Mg-Zn-Ce alloys show that the basal poles are split in RD direction even at 300 °C. The minimum basal texture intensity is exhibited by Mg-1Zn-1Ce at both 300 °C and 450 °C, which has the highest Ce/Zn ratio.

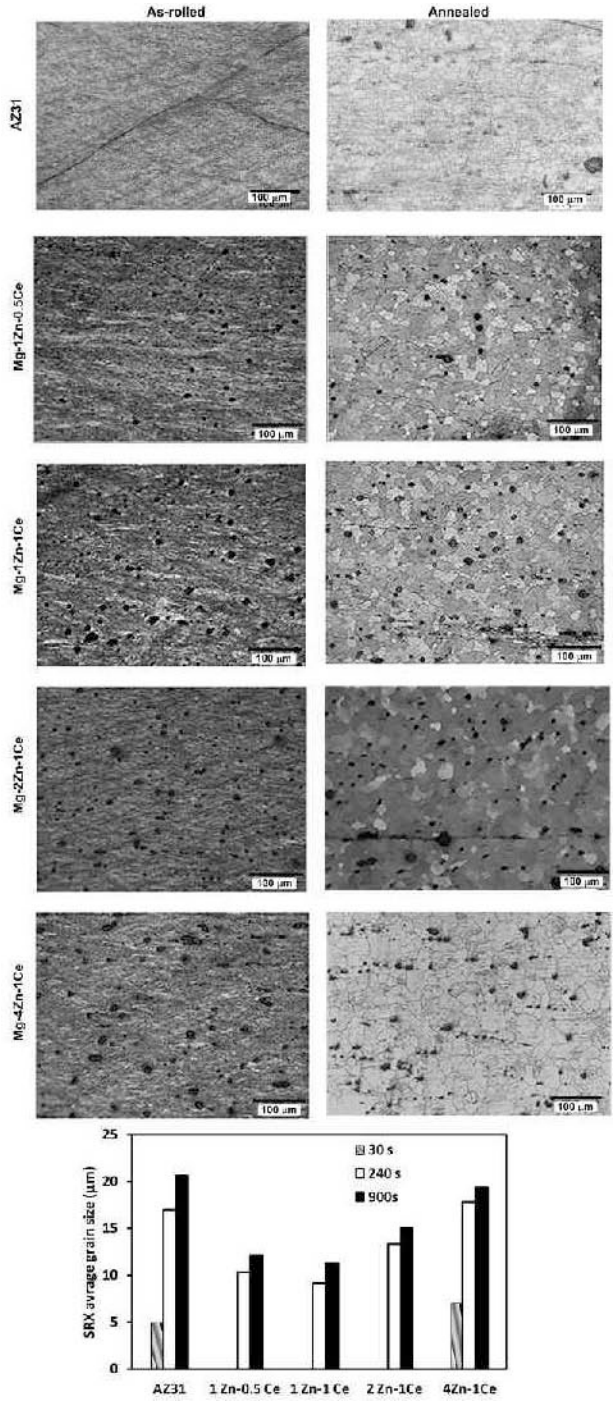

Fig. 1 The microstructure of the finish rolled samples of the Mg-Zn-Ce alloys rolled at 300°C in the as rolled condition (left side) and annealed for 15 min at 450°C (right side). The effect of

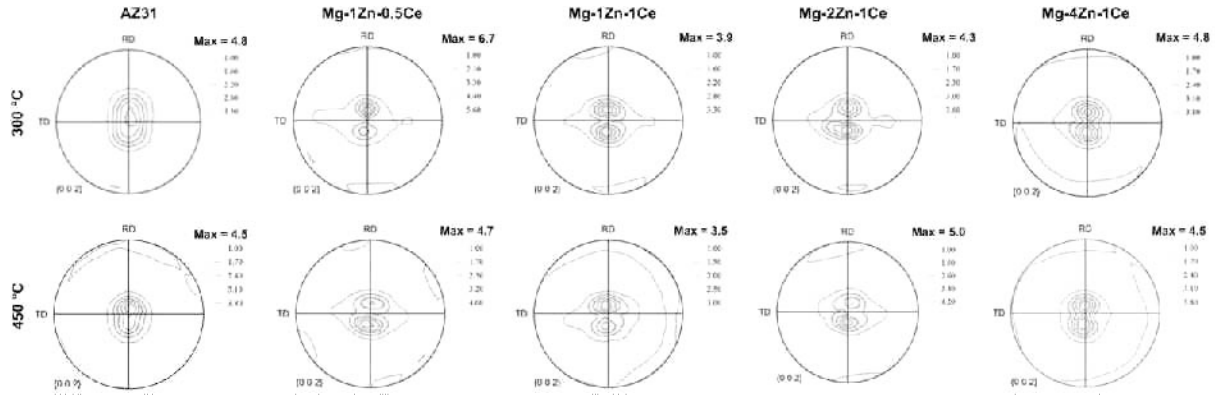

Fig. 2 {0002} pole figure of the finish rolled samples for AZ31 and Mg-Zn-Ce alloys at two temperatures of 300°C and 450°C in the as-rolled condition.

Microstructure and texture evolution during annealing

To study the effect of the Ce/Zn ratio on the texture and microstructure evolution during annealing, Mg-1Zn-1Ce and Mg-4Zn-1Ce were selected as the highest and lowest Ce/Zn ratio respectively and compared with AZ31. The texture evolution during annealing at 300 °C for different annealing times is shown in Fig 3. As can be seen, after 60 min annealing, all the textures are weaker than the as-rolled textures regardless of alloy. However, the three alloys show two different types of texture evolution during annealing. AZ31 and Mg-4Zn-1Ce are similar and they both exhibit a sudden decrease in texture intensity after 30 s anneal, followed by a plateau trough and then an increase at 6 min for AZ31 and 10 min for Mg-4Zn-1Ce. Both alloys reach a maximum after about 30 min, which plateaus with longer times. AZ31 exhibits much higher intensities outside the trough, but the trough intensities are similar. Mg-1Zn-1Ce, on the other hand, exhibits a steady decrease after 60 s annealing; after 60 min, the texture intensity is lower than the trough values of the other alloys. After about 20 min annealing the texture intensity is does not change significantly.

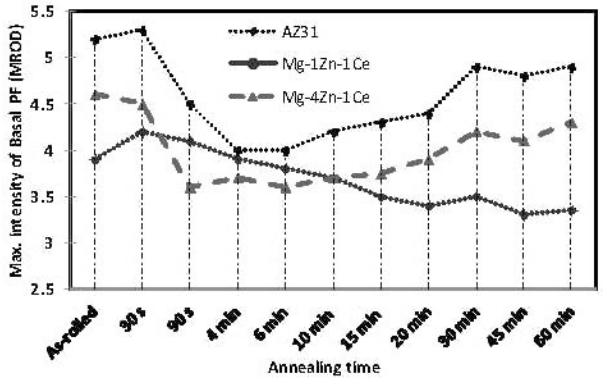

Fig 3. The intensity (in multiples random of distribution or MROD) in the basal pole figures plotted as a function annealing time at 300 °C for the AZ31, Mg-1Zn-1Ce and Mg-4Zn-1Ce alloys finish rolled at 300 °C.

The microstructure evolution with annealing time is shown in Fig. 4. Following annealing up to 90 s, both AZ31 and Mg-4Zn-1Ce are fully recrystallized, whereas Mg-1Zn-1Ce is not. For both AZ31 and Mg-4Zn-1Ce, full recrystallization coincides approximately with the beginning of the sharp decrease in hardness, as indicated by the arrows on the graph. After 10 min annealing, both AZ31 and Mg-4Zn-1Ce exhibit a bimodal microstructure consisting of small and large grains, but generally having a size less than 10 μm. The hardness value after this time follows a plateau trough. The slightly further decrease in hardness and further grain growth as well as evidence of abnormal grain growth can be observed in the microstructure (arrowed) after increasing the annealing time to 60 min.

On the other hand for Mg-1Zn-1Ce, there is no sign of recrystallization in the microstructure up to 4 min annealing time. After 60 min annealing, the recrystallized grain size is smaller in comparison with the other two alloys and there is no sign of abnormal grain growth in the microstructure.

Texture evolution of AZ31 and Mg-4Zn-1Ce during annealing

In the case of AZ31 deformed at 300 °C with reduction ≈60% in a single pass, there were few signs of DRX after rolling. The deformed microstructure was completely replaced by SRXed grains after 90s annealing at 300 °C, (Fig. 4). At this stage, as was seen in Fig. 3, the maximum intensity also decreases from 5.3 to 4.5 multiples random of distribution (MROD). Therefore; it seems that decrease in texture intensity after 90 s annealing time in the AZ31 is corresponding to recovery or the beginning of SRX.

As was seen in Fig. 4, the new SRX grains started forming at bands. Sandlobes et al. [15] reported that such shear bands contain a high volume fraction of compression and secondary twins.

The orientation changes associated with twin recrystallization are not understood well yet. In the previous work of the authors [17], the misorientation of new recrystallized grains on secondary twin (S-twins) was investigated with respect to the primary twin hosts in partially recrystallized twins. It was concluded that the high frequency of ≈ 77° misorientation illustrated that the orientations of the recrystallized grains are closer to secondary (tension twin 86°), rather than of the primary, compression twins (C-twins). Therefore; the orientation of recrystallized grains has much more wider distribution than that of initial basal parent. For this reason, it seems that rapid recrystallization on twins contributes to the texture weakening during first 90 s of annealing for both AZ31 and Mg-4Zn-1Ce.

After the initial sudden drop for both alloys the maximum basal intensity reach to a plateau trough. By further annealing the SRX grain size increase in normal way up to about 10 min for both alloys. After this time some grains start to grow in abnormally, as can be seen in the microstructure of AZ31 annealed for 10 min in Fig.4.

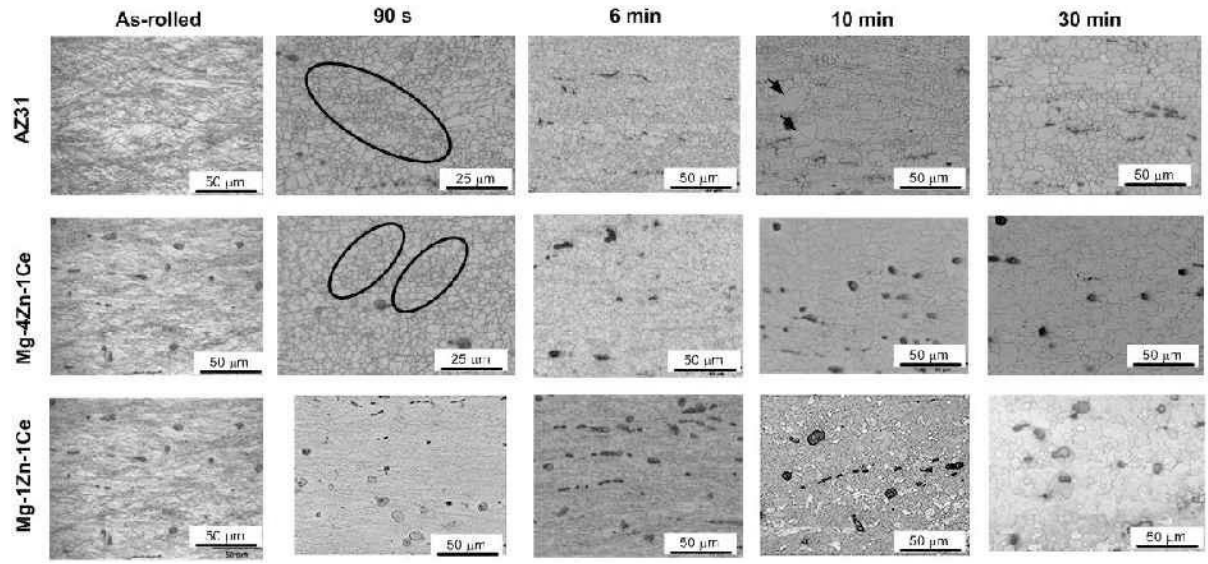

Fig. 4 Optical micrographs for AZ31, Mg-4Zn-1Ce and Mg-1Zn-1Ce rolled at 300 °C followed by annealing at 300 °C for different times

Close inspection of the EBSD data in the annealed samples of AZ31 at different times revealed that the size distribution of recrystallized grains exhibits a principal peak representing the average size, and for samples annealed more than 10 min, secondary peaks can be detected (Fig 5).

As the PF for the grains larger than the average shows in Fig.5, the orientation of these recrystallized grains shows more basal orientation. Therefore; it seems by increasing the annealing time the area fraction of these basal grains increases and the basal intensity increased.

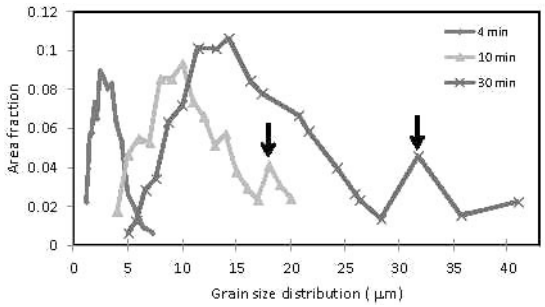

Fig. 5 Grain size distribution for static recrystallized grains in AZ31 annealed for 4, 10 and 60 min at 300 °C. The samples rolled at 300 °C.

Texture evolution of Mg-1Zn-1Ce during annealing

As was seen in Fig. 3 the basal texture is continuously dropping during annealing. By adding Ce to the alloys, the DRX and SRX mechanisms can be influenced by changing both nucleation and growth. As was observed in the as-deformed microstructure in Fig. 4 and also reported by other researchers [4, 8, 13], by adding rare earth elements more C-twins and S-twins form in the material. By increasing the annealing time the volume fraction of SRX increases, which corresponds to weakening of the basal texture and an increase in the inclination of the basal pole toward the rolling direction (RD) from ~12° to ~25°. Close inspection of Fig. 4 shows that, although there appears to be a continuous drop of texture intensity, in fact the intensity effectively reaches a plateau at 20 min, which corresponds to the end of SRX in this alloy (Fig. 4). Therefore it seems that the different SRX rates of these three alloys is the main reason for the different texture weakening behaviour as will be explained in more detail in following section.

Possible texture weakening mechanism for Mg-1Zn-1Ce

To study the SRX mechanism in this alloy a rough rolled sample, which was not dynamically recrystallized and had large grains, was annealed at different times. The microstructure and texture evolution were tracked for the same area. As can be seen in Fig. 6a, the rough rolled microstructure of Mg-1Zn-1Ce contains many twins. These twins are zones of deformation localization and can pass through several grains and become deformation bands, as also mentioned in the recent study of Sandlobes et al. [23]. After 4 min annealing at 300°C, new non basal grains recrystallized in bands and individual twins. Figure 6b depicts the growth of one SRX grain (arrow) into a basal parent region, and the initial twin nucleation site of this grain is shown in Fig. 6a. As is seen in Fig. 6b and c, this grain coarsened and some parts expanded into a basal parent grain of the basal matrix. The growth of the highlighted grains continues with further annealing (Fig. 6 d). Static recrystallization also occurs at basal parent grains, giving rise to grains exhibiting mostly basal orientations, as is illustrated by the grains numbered 1 and 2 in Figs. 6 b, c and d. As shown in Fig. 6 during the progress of SRX, the intensity of the basal texture continues to drop.

Stanford et al [12] suggested that the dislocation/solute interactions are an important aspect in the rare earth effect on the texture. They reported that Ce and La are the most effective texture modifiers because of their large atomic radii. It was suggested that there is a strong interaction of RE solutes with

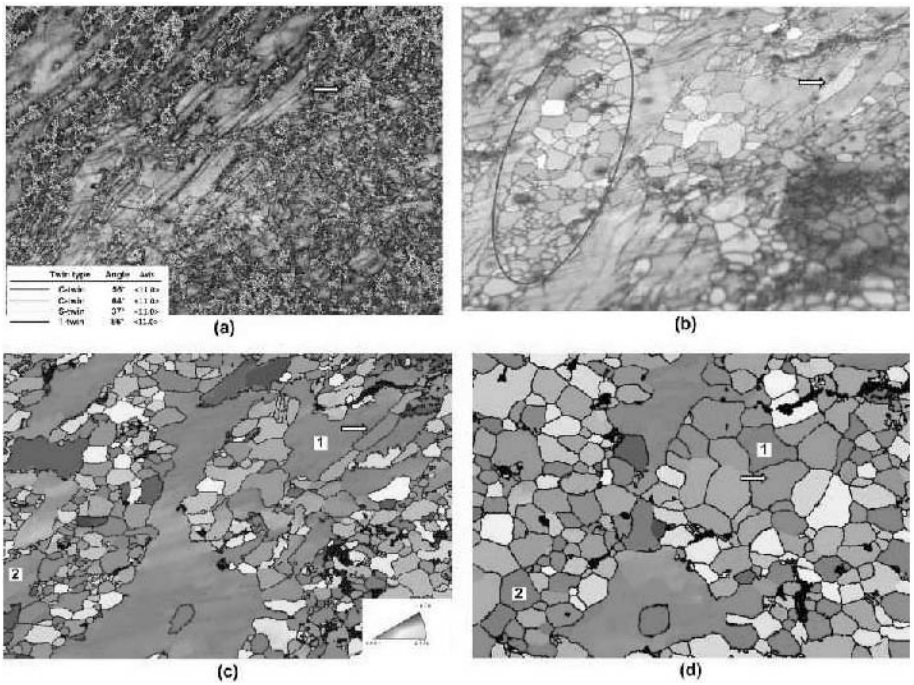

Fig. 6 EBSD results for the rough rolled Mg-1Zn-1Ce annealed for different time (a) IQ map of the as-rolled material with the boundaries corresponding to different twins (Color figure online) (b) IQ map for the sample anneal for 4 min and (c) IPF map for the sample anneal for 4 and (d)10 min. Twin nucleation site (a) and the growth of this grain during annealing is arrowed (b, c and d).

dislocations and boundaries in magnesium-based alloys [4].

To study the effect of Zn content on the solubility of Ce in magnesium, thermodynamic calculations were carried out using the FactSageTM thermodynamic software (Fig. 7). Based on these results, by increasing the Zn in the Mg-Zn-Ce alloy systems, the solubility of Ce in Mg decreases. This was supported by the observed increase in Ce-rich precipitates in Mg-4Zn-1Ce. Therefore, it can be concluded that the grain boundary mobility increased in the alloys with lower Ce/Zn ratio. Therefore, it seems that higher solubility of Ce in Mg-1Zn-1Ce magnesium may be a key reason for the weaker basal texture in both deformed and recrystallized conditions. It was hypothesised, in the previous work of the author, that by suppressing the DRX, the deformation cannot be accommodated in the soft DRX region; instead deformation is accommodated by compression and double twinning in basal parent grains, leading to the formation of deformation bands [24].

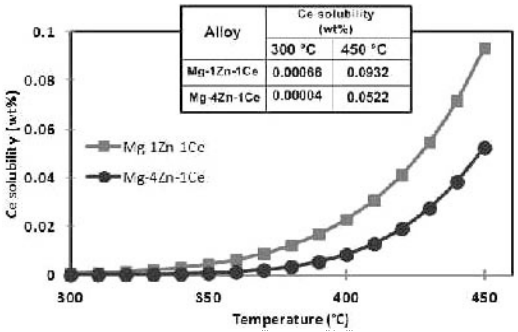

Fig. 7 Calculated Ce solubility vs. temperature for Mg-1Zn-1Ce and Mg-4Zn-1Ce alloys using FactSage^{TM} thermodynamic software.

Conclusions

Microstructure and texture development in four Mg-Zn-Ce alloys and Mg-3Al-1Zn were studied following rolling and subsequent isothermal annealing. The main results are summarized as follows.

-The addition of Ce weakens the basal texture in both the as-hot rolled and annealed conditions. This appears to be related to an increase in deformation twins during hot rolling, which is due to Ce in solid solution.

Increasing Zn decreases Ce in solid solution. Hence the alloy with the higher Ce/Zn ratio exhibited weaker basal textures.

The maximum intensity of basal pole figures decreases as static recrystallization progresses for all the alloys. This probably corresponds to the formation of SRX grains with wider orientation spread at twins and deformation bands.

The basal texture intensifies after the end of SRX because of abnormal grain coarsening of some grains with orientation close to basal.

Acknowledgments

The authors would like to thank Mr Miyamoto, Mr Hattori and Mr Muraoka from his kind support for rolling experiments at Osaka University. Thanks to Pierre Vermette at McGill University and Amjad Javaid, Howard Webster and David Saleh in the Natural Resources Canada's CANMET materials technology laboratory for casting the alloys. This study was supported by the NSERC Magnesium Strategic Research Network (MagNET) and MEDA Fellowship from Faculty of Engineering of McGill University.

References

[1] H.B. M. Avedesian, *ASM specialty handbook. Magnesium and magnesium alloys.* (ed., Materials Park, Ohio: ASM International, 2000).

[2] M. Shamsi, M. Sanjari, A.Z. Hanzaki, "Study of fractional softening of AZ31 magnesium alloy under multistage hot deformation," *Materials Science and Technology*, 25 (2009) 1039-1045.

[3] T. Al-Samman, G. Gottstein, "Dynamic recrystallization during high temperature deformation of magnesium," *Materials Science and Engineering A*, 490 (2008) 411-420.

[4] S.R. Agnew, M.H. Yoo, C.N. Tomé, "Application of texture simulation to understanding mechanical behavior of Mg and solid solution alloys containing Li or Y," *Acta Materialia*, 49 (2001) 4277-4289.

[5] L.W.F. Mackenzie, M. Pekguleryuz, "The influences of alloying additions and processing parameters on the rolling microstructures and textures of magnesium alloys," *Materials Science and Engineering: A*, 480 (2008) 189-197.

[6] A. Styczynski, C. Hartig, J. Bohlen, D. Letzig, "Cold rolling textures in AZ31 wrought magnesium alloy," *Scripta Materialia*, 50 (2004) 943-947.

[7] K. Hantzsche, J. Bohlen, J. Wendt, K.U. Kainer, S.B. Yi, D. Letzig, "Effect of rare earth additions on microstructure and texture development of magnesium alloy sheets," *Scripta Materialia*, 63 (2010) 725-730.

[8] J. Bohlen, M.R. Nürnberg, J.W. Senn, D. Letzig, S.R. Agnew, "The texture and anisotropy of magnesium-zinc-rare earth alloy sheets," *Acta Materialia*, 55 (2007) 2101-2112.

[9] R. Cottam, J. Robson, G. Lorimer, B. Davis, "Dynamic recrystallization of Mg and Mg-Y alloys: Crystallographic texture development," *Materials Science and Engineering: A*, 485 (2008) 375-382.

[10] L.W.F. Mackenzie, M.O. Pekguleryuz, "The recrystallization and texture of magnesium-zinc-cerium alloys," *Scripta Materialia*, 59 (2008) 665-668.

[11] N. Stanford, "Micro-alloying Mg with Y, Ce, Gd and La for texture modification--A comparative study," *Materials Science and Engineering: A*, 527 (2010) 2669-2677.

[12] H. Yan, S.W. Xu, R.S. Chen, S. Kamado, T. Honma, E.H. Han, "Twins, shear bands and recrystallization of a Mg-2.0%Zn-0.8%Gd alloy during rolling," *Scripta Materialia*, 64 (2011) 141-144.

[13] E.A. Ball, P.B. Prangnell, "Tensile-compressive yield asymmetries in high strength wrought magnesium alloys," *Scripta Metallurgica et Materiala*, 31 (1994) 111-116.

[14] L.W.F. Mackenzie, G.W. Lorimer, F.J. Humphreys, T. Wilks, "Recrystallization behaviour of two magnesium alloys," *Journal*, 467-470 (2004) 477-482.

[15] N. Stanford, M.R. Barnett, "The origin of "rare earth" texture development in extruded Mg-based alloys and its effect on tensile ductility," *Materials Science and Engineering: A*, 496 (2008) 399-408.

[16] T. Al-Samman, X. Li, "Sheet texture modification in magnesium-based alloys by selective rare earth alloying," *Materials Science and Engineering A*, 528 (2011) 3809-3822.

[17] H. Kon, T. Sakai, H. Utsunomiya, S. Minamiguchi, "Deformation and texture evolution during high-speed rolling of AZ31 magnesium sheets," *Materials Transactions*, 48 (2007) 2023-2027.

[18] H. Utsunomiya, T. Sakai, S. Minamiguchi, H. Koh, "High-speed heavy rolling of magnesium alloy sheets," *Journal*, 2006 (2006) 201-204.

[19] G. Hamada, T. Sakai, H. Utsunomiya, "Effect of rolling speed on deformability and microstructure in rolling of AZ31B magnesium alloy," *Journal*, 89-91 (2010) 227-231.

[20] T. Sakai, Y. Watanabe, H. Utsunomiya, "Microstructure and texture of AZ80 magnesium alloy sheet rolled by high speed warm rolling," *Journal*, 618 619 (2009) 483-486.

[21] R.K. Mishra, A.K. Gupta, P.R. Rao, A.K. Sachdev, A.M. Kumar, A.A. Luo, "Influence of cerium on the texture and ductility of magnesium extrusions," *Scripta Materialia*, 59 (2008) 562-565.

[22] S. Sandlöbes, S. Zaefferer, I. Schestakow, S. Yi, R. Gonzalez-Martinez, "On the role of non-basal deformation mechanisms for the ductility of Mg and Mg-Y alloys," *Acta Materialia*, 59 (2011) 429-439.

[23] Y.B. Chun, J. Geng, N. Stanford, C.H.J. Davies, J.F. Nie, M.R. Barnett, "Processing and properties of Mg–6Gd–1Zn–0.6Zr: Part 1 – Recrystallisation and texture development," *Materials Science and Engineering: A*, 528 (2011) 3653-3658.

[24] H. Li, E. Hsu, J. Szpunar, H. Utsunomiya, T. Sakai, "Deformation mechanism and texture and microstructure evolution during high-speed rolling of AZ31B Mg sheets," *Journal of Materials Science*, 43 (2008) 7148-7156.

[25] S.L. Couling, F. Pashak, L. Sturkey, *Trans. ASM*, 51 (1959) 94-107.

[26] B.H. Lee, W. Bang, S. Ahn, C.S. Lee, "Effects of temperature and strain rate on the high-temperature workability of strip-cast Mg-3Al-1Zn alloy," *Metallurgical and Materials Transactions A: Physical Metallurgy and Materials Science*, 39 A (2008) 1426-1434.

[27] S. Yi, I. Schestakow, S. Zaefferer, "Twinning-related microstructural evolution during hot rolling and subsequent annealing of pure magnesium," *Materials Science and Engineering: A*, 516 (2009) 58-64.